Extensive weight loss can reduce immune age by altering IgG N-glycosylation

Valentina L Greto[1]*, Ana Cvetko[2]*, Tamara Štambuk[3]*, Niall J Dempster[4], Domagoj Kifer[2], Helena Deriš[3], Ana Cindrić[3], Frano Vučković[3], Mario Falchi[5], Richard S Gillies[6], Jeremy W Tomlinson[4], Olga Gornik[2,3], Bruno Sgromo[6], Tim D Spector[5], Cristina Menni[5]*, Alessandra Geremia[1]*, Carolina V Arancibia-Cárcamo[1]*, Gordan Lauc[2,3]*

[1]Translational Gastroenterology Unit and NIHR Oxford Biomedical Research Centre, Nuffield Department of Medicine, University of Oxford, United Kingdom

[2]Faculty of Pharmacy and Biochemistry, University of Zagreb, Zagreb, Croatia

[3]Genos Glycoscience Research Laboratory, Zagreb, Croatia

[4]Oxford Centre for Diabetes and NIHR Oxford Biomedical Research Centre, Endocrinology and Metabolism, Radcliffe Department of Medicine, University of Oxford, United Kingdom

[5]The Department of Twin Research, King's College London, St Thomas' Hospital, London, United Kingdom

[6]Department of Upper GI Surgery, Oxford University Hospitals, United Kingdom

*The authors equally contributed to this work

Corresponding author:

Gordan Lauc

glauc@pharma.hr

Faculty of Pharmacy and Biochemistry, University of Zagreb

A. Kovačića 1, 10 000 Zagreb, Croatia

ABSTRACT

Background

Obesity represents a global health threat, and is associated not only with exponentially increased cardiometabolic morbidity and mortality, but with adverse clinical outcomes in patients infected with SARS-CoV-2 as well. Enzymatic attachment of complex oligosaccharides to proteins (glycosylation) is highly responsive to numerous (patho)physiological conditions and ageing, which is perhaps best exemplified on IgG. The prospect of immune age reduction, by reverting induced glycosylation changes through metabolic intervention, opens many possibilities. Herein, we have investigated whether weight loss interventions affect inflammation- and ageing-related glycosylation alterations, in a longitudinal cohort of bariatric-surgery patients. To support potential findings, BMI-related glycosylation changes were monitored in a longitudinal TwinsUK cohort.

Methods

IgG and plasma N-glycans were chromatographically profiled in 37 obese patients, subjected to low-calorie diet and then to bariatric surgery, across multiple timepoints. Similarly, plasma glycome was analysed in 1,680 TwinsUK participants and longitudinally monitored during a 20-year follow-up.

Findings

Low-calorie diet induced marked increase in low branched and significant decrease in highly branched, more complex plasma N-glycans – the change opposite to the one typically observed in inflammatory conditions. Bariatric surgery resulted in extensive, gradual alterations in IgG glycome, that accompanied progressive weight loss during one year follow-up. We observed significant increase in digalactosylated and sialylated, and substantial decrease in agalactosylated and core fucosylated IgG glycans. In general, such IgG glycan profile is associated with a younger biological age and reflects enhanced anti-inflammatory IgG potential. The TwinsUK cohort replicated weight loss-associated agalactosylation decrease and digalactosylation increase, estimated through BMI decrease over a 20-year-period.

Interpretation

Altogether, these findings highlight that weight loss substantially affects both plasma and IgG N-glycosylation, resulting in improved biological and immune age.

GRAPHICAL ABSTRACT

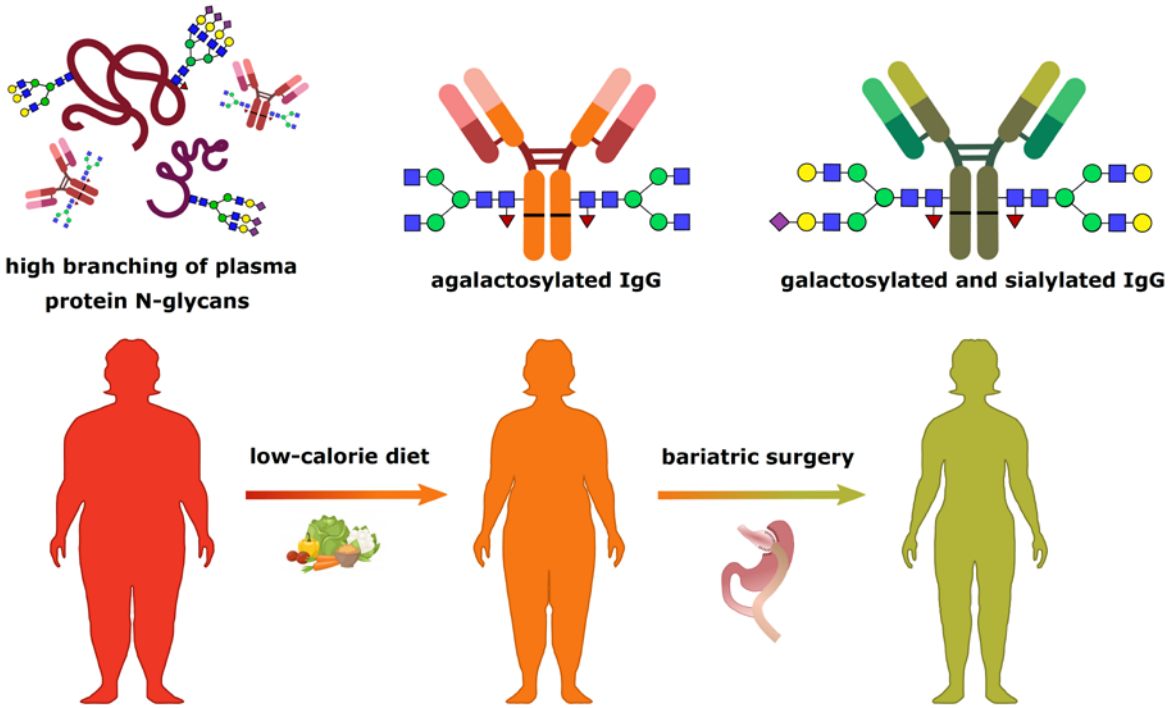

HIGHLIGHTS

- Obesity is associated to circulating pro-inflammatory high branched N-glycans and IgG agalactosylation
- High branching of N-glycans from total plasma proteins decreases after 3-week low-calorie diet
- IgG galactosylation and sialylation increase after bariatric surgery-induced weight loss
- Decrease of BMI over time is associated to increased IgG galactosylation and a reduction of biological age

KEYWORDS

N-glycosylation; bariatric surgery; weight loss; imunoglobulin G; COVID-19; biological age

55 **INTRODUCTION**

56 The global prevalence of obesity has risen dramatically, to the point that it is now considered
57 a pandemic (1). In the current collision with the emergent coronavirus disease (COVID-19
58 pandemic), there is a strong association of obesity and older age with COVID-19 complications
59 and severity (2). Moreover, US Centre for Disease Control and Prevention recently reported
60 that obesity represents the highest risk factor for COVID-19 mortality in people younger than
61 65 years (3). According to the World Health Organization, over 650 million individuals are
62 obese, accounting for 13% of the world's adult population. Obesity confers a risk for metabolic
63 syndrome, contributing to type 2 diabetes and cardiovascular disease (CVD) development (4).
64 Metabolic syndrome is linked to a chronic systemic low-grade inflammation, which
65 contributes to the aging of the immune system denoted as inflammaging (5,6). Obesity-
66 related inflammaging results in impaired innate and adaptive immune function, and is
67 characterized by high serum levels of IL-6, TNF-α and CRP (7). Moreover, this persistent
68 inflammatory state may potentially lead to increased viral shedding and to delayed, blunted
69 antiviral responses to SARS-CoV-2 infection (8,9).

70 Changes in protein N-glycosylation are one of the hallmarks of inflammaging (6,9). The human
71 circulating N-glycome represents the entire set of glycans that are covalently attached to
72 plasma proteins through a nitrogen on an asparagine residue. N-glycans are essential for life
73 and are involved in many physiological processes (10), including signal transduction, protein
74 trafficking and folding, receptor regulation and cell adhesion. Glycosylation has a fundamental
75 role in the innate and adaptive immune responses, accentuated by the fact that all five classes
76 of immunoglobulins (Ig) bear N-glycans. In this regard, IgG is probably the most investigated
77 glycoprotein, whose effector functions are controlled by its Fc-bound glycans (11).

78 Inter-individual differences in the pace of biological ageing is an intriguing concept that tries
79 to explain why some people stay healthy until very late chronological age, while others age
80 faster and have shorter life expectancy. The same may apply for the risk of severe COVID-19.
81 Progressive age-related changes of IgG glycosylation have been extensively studied (10,12,13),
82 and the GlycanAge model has been proposed to express the difference between chronological
83 ageing and IgG glycome ageing (14). The "age" of the IgG glycome might be estimated through
84 the levels of agalactosylated species, which are increasing with ageing and are associated with
85 enhanced immune activation (15). The opposite applies for digalactosylated IgG glycoforms,
86 which are usually related to a younger age. Besides age-related changes, specific IgG

87 glycosylation patterns have been already associated with CVD risk score and subclinical
88 atherosclerosis in two large independent UK cohorts (16). Moreover, a prospective follow-up
89 of the EPIC-Potsdam cohort confirmed that changes in plasma N-glycome composition are
90 predictive of future CVD events, with comparable predictive power to the American Heart
91 Association (AHA) score in men and even better predictive power in women (17). The link
92 between an "old", proinflammatory IgG N-glycome and hypertension has also been
93 profoundly studied (18–20), and similar IgG glycosylation patterns were associated with
94 increased body mass index (BMI) and measures of central adiposity (21,22).
95 Studies on mouse models further corroborate the importance of differential IgG glycoforms
96 in CVD pathogenesis. Namely, it has been shown that hyposialylated IgG (corresponding to an
97 "old" IgG glycome) can induce obesity-related hypertension and insulin resistance in B-cell-
98 deficient mice, through activation of the endothelial FcγRIIB (23,24). These findings indicate
99 that the IgG N-glycome could represent more than a biomarker of inflammation and aging,
100 since distinctive IgG glycoforms act as effector molecules in certain pathologies. Furthermore,
101 supplementation with *N*-acetylmannosamine (ManNAc), a precursor of sialic acid, protects
102 obese mice from hypertension and insulin resistance induction by reverting an "old" IgG N-
103 glycome into a "young" one (24,25). However, studies exploring the possibilities of converting
104 an "old" IgG glycome into a "young" one by metabolic intervention in humans are limited. Of
105 note, only one small study indicated that high-intensity interval training can "rejuvenate" the
106 IgG N-glycome (26).
107 Finally, severe obesity can be resolved only through bariatric surgery and subsequent weight
108 loss (27). The resulting weight loss impacts energy balance and metabolism, contributing to
109 the increased insulin response, improved glycaemic control and reduction of total body fat,
110 leading to decreased CVD risk and mortality (28). In this study we aimed to determine whether
111 weight loss affects glycan markers related to inflammation and ageing, in a longitudinally-
112 monitored cohort of obese individuals undergoing low-calorie diet and then bariatric surgical
113 interventions. In order to support potential findings, we also investigated the BMI-related
114 glycosylation changes in a longitudinal TwinsUK cohort. The analysis of samples obtained from
115 the largest longitudinal twins cohort in the UK allowed us to observe the changes of BMI in
116 relation to the IgG N-glycosylation alterations over time.
117
118

119 **METHODS**

120 **Study populations**

121 *Bariatric cohort*. The cohort included 37 participants, recruited at Oxford University Hospitals
122 to the Gastrointestinal Illnesses study (Ref: 16/YH/0247). All patients were characterised by
123 metabolic status and medical history. Bariatric patients were considered eligible in accordance
124 to National Institute for Health and Care Excellence (NICE) and local guidelines. The choice of
125 bariatric operation was decided according to the Oxford Bariatric Unit regular practice.
126 Patients with a history of alcoholism and/or ongoing anticoagulant treatment were excluded.
127 Patients were also excluded in case of pregnancy, active substance abuse or uncontrolled
128 psychiatric condition including eating disorders. Participants were sampled at baseline and
129 subjected to 3-week low calorie carbohydrate-restricted diet (900 cal, maximum 100 g of
130 carbohydrates per day), followed by bariatric surgery. The sequential follow-up timepoints
131 included the day of the surgery (baseline), after 6.54 ± 3.4 months (mean ± IQR) and 12.47 ±
132 6.55 months post-op. Characteristics of the bariatric cohort are shown in Table 1.

133 **Table 1 Demographic characteristics of the bariatric cohort**

Characteristics	*Bariatric cohort*				
Total No. of participants (N)	37				
No. of participants Sleeve Gastrectomy (SG), N (%)	25 (68%)				
No. Roux-en-Y Gastric Bypass RYGB N (%)	12 (32%)				
No. of participants each timepoint (N)	Pre-op low-calorie diet		Time of surgery	1st post-op timepoint	2nd post-op timepoint
	8		37	30	24
BMI* each timepoint, mean ± SD, kg/m2	Before diet	End of diet	Time of surgery	1st post-op timepoint	2nd post-op timepoint
	48.53 ± 4.13	46.60± 4.21	46.21 ± 4.75	36.01 ± 5.07	32.82 ± 5.17
Female, sex, N (%)	33 (89%)				
Type 2 diabetes, N (%)	6 (16%)				

134
135 *BMI reference values: <18.5 (underweight), 18.5–24.9 (normal weight), 25–29.9
136 (overweight), >30 (obese).
137
138 *TwinsUK cohort.* We have analysed a total of 6,032 plasma samples from 2,146 participants of
139 the TwinsUK study, collected at multiple timepoints over a 20 year-period (29). These included
140 1,865 individuals sampled at 3 timepoints, 156 individuals sampled at 2 timepoints and 125
141 individuals sampled only once. Following the plasma N-glycome analysis, glycan data

142 underwent quality control (see *Statistical analysis* section), which decreased the dataset to
143 5,889 samples (measurements). Out of these 5,889 measurements, we have proceeded with
144 statistical analysis on a subset of 3,742 samples (measurements) which had information on
145 BMI available. Description of the TwinsUK cohort is provided in Table 2.

146 **Table 2 Demographic characteristics of the TwinsUK cohort**

Characteristics	*TwinsUK cohort (BMI subset)*
No. of participants (N)	1,680
No. of glycan measurements (N)	3,742
Baseline age, mean ± SD, years	53.23 ± 10.86
Follow up time, mean ± SD, years	7.90 ± 5.66
Female sex, N (%)	1,680 (100)
Baseline BMI, mean ± SD, kg/m^2	25.45 ± 4.53

147

148 **Ethical statement**

149 Ethical approval for the study was obtained by the National Research Ethics Committees of
150 the UK National Health Service (NHS) under the reference number 16/YH/0247. All individuals
151 participating in this study gave written informed consent. The TwinsUK study was approved
152 by NRES Committee London–Westminster, and all twins provided informed written consent.

153 **N-glycome analysis**

154 *Isolation of IgG from human plasma*

155 IgG was isolated from plasma samples by affinity chromatography as described previously
156 (30). In brief, IgG was isolated in a high-throughput manner, using 96-well protein G
157 monolithic plates (BIA Separations, Slovenia), starting from 100 µl of plasma. Plasma was
158 diluted 7× with phosphate buffered saline (PBS; Merck, Germany) and applied to the protein
159 G plate. IgG was eluted with 1 ml of 0.1 M formic acid (Merck, Germany) and immediately
160 neutralized with 1 M ammonium bicarbonate (Acros Organics, USA).

161 *N-glycan release from IgG and total plasma proteins*

162 Isolated IgG samples were dried in a vacuum centrifuge. After drying, IgG was denatured with
163 the addition of 30 µl of 1.33% SDS (w/v) (Invitrogen, USA) and by incubation at 65 °C for 10
164 min. Plasma samples (10 µl) were denatured with the addition of 20 µl of 2% (w/v) SDS
165 (Invitrogen, USA) and by incubation at 65 °C for 10 min. From this point on, the procedure was

166 identical for both IgG and plasma samples. After denaturation, 10 µl of 4% (v/v) Igepal-CA630
167 (Sigma Aldrich, USA) was added to the samples, and the mixture was shaken 15 min on a plate
168 shaker (GFL, Germany). N-glycans were released with the addition of 1.2 U of PNGase F
169 (Promega, USA) and overnight incubation at 37 °C.

170 *Fluorescent labelling and HILIC SPE clean-up of released N glycans*

171 The released N-glycans were labelled with 2-aminobenzamide (2-AB). The labelling mixture
172 consisted of 2-AB (19.2 mg/ml; Sigma Aldrich, USA) and 2-picoline borane (44.8 mg/ml; Sigma
173 Aldrich, USA) in dimethyl sulfoxide (Sigma Aldrich, USA) and glacial acetic acid (Merck,
174 Germany) mixture (70:30 v/v). To each sample 25 µl of labelling mixture was added, followed
175 by 2 h incubation at 65 °C. Free label and reducing agent were removed from the samples
176 using hydrophilic interaction liquid chromatography solid-phase extraction (HILIC-SPE). After
177 incubation samples were brought to 96% of acetonitrile (ACN) by adding 700 µl of ACN (J.T.
178 Baker, USA) and applied to each well of a 0.2 µm GHP filter plate (Pall Corporation, USA).
179 Solvent was removed by application of vacuum using a vacuum manifold (Millipore
180 Corporation, USA). All wells were prewashed with 70% ethanol (Sigma-Aldrich, St. Louis, MO,
181 USA) and water, followed by equilibration with 96% ACN. Loaded samples were subsequently
182 washed 5× with 96% ACN. N-glycans were eluted with water and stored at − 20 °C until usage.

183 *Hydrophilic interaction liquid chromatography of N glycans*

184 Fluorescently labelled N-glycans were separated by hydrophilic interaction liquid
185 chromatography (HILIC) on Acquity UPLC H-Class instrument (Waters, USA) consisting of a
186 quaternary solvent manager, sample manager and a fluorescence detector, set with excitation
187 and emission wavelengths of 250 and 428 nm, respectively. The instrument was under the
188 control of Empower 3 software, build 3471 (Waters, Milford, USA). Labelled N-glycans were
189 separated on a Waters BEH Glycan chromatography column, with 100 mM ammonium
190 formate, pH 4.4, as solvent A and ACN as solvent B. In the case of IgG N-glycans, separation
191 method used linear gradient of 75–62% acetonitrile at flow rate of 0.4 ml/min in a 27-min
192 analytical run. For plasma protein N-glycans separation method used linear gradient of 70–
193 53% acetonitrile at flow rate of 0.561 ml/min in a 25-min analytical run. The system was
194 calibrated using an external standard of hydrolysed and 2-AB labelled glucose oligomers from
195 which the retention times for the individual glycans were converted to glucose units (GU).
196 Data processing was performed using an automatic processing method with a traditional
197 integration algorithm after which each chromatogram was manually corrected to maintain

198 the same intervals of integration for all the samples. The chromatograms were all separated
199 in the same manner into 24 peaks (GP1– GP24) for IgG N-glycans and 39 peaks (GP1–GP39)
200 for plasma protein N-glycans and are depicted in Supplementary Figure 1 and Supplementary
201 Figure 2, respectively. Detailed description of glycan structures corresponding to each glycan
202 peak is presented in Supplementary Table 1. Glycan peaks were analysed based on their
203 elution positions and measured in glucose units, then compared to the reference values in the
204 "GlycoStore" database (available at: https://glycostore.org/) for structure assignment. The
205 amount of glycans in each peak was expressed as a percentage of the total integrated area.
206 For IgG glycans, in addition to 24 directly measured glycan traits, 8 derived traits were
207 calculated, while for plasma glycans, in addition to 39 directly measured glycan traits, 16
208 derived traits were also calculated. These derived traits average particular glycosylation
209 features, such as galactosylation, fucosylation, bisecting GlcNAc, and sialylation. Formulas for
210 IgG and plasma protein N-glycan derived traits for bariatric cohort are presented in
211 Supplementary Table 2 and Supplementary Table 3, respectively. Derived trait calculations for
212 TwinsUK cohort are presented in Supplementary Table 4.

213 **Statistical analysis**

214 *Bariatric cohort.* In order to remove experimental variation from the measurements,
215 normalization and batch correction were performed on the UPLC glycan data. To make
216 measurements across samples comparable, normalization by total area was performed. Prior
217 to batch correction, normalized glycan measurements were log-transformed due to right-
218 skewness of their distributions and the multiplicative nature of batch effects. Batch correction
219 was performed on log-transformed measurements using the ComBat method (R package sva
220 (31), where the technical source of variation (which sample was analysed on which plate) was
221 modelled as batch covariate. To correct measurements for experimental noise, estimated
222 batch effects were subtracted from log-transformed measurements.

223 Longitudinal analysis of patient samples through their observation period was performed by
224 implementing a linear mixed effects model, where time was modelled as fixed effect, while
225 the individual ID was modelled as random effect. Prior to the analyses, glycan variables were
226 all transformed to standard Normal distribution by inverse transformation of ranks to
227 Normality (R package "GenABEL", function rntransform). Using rank transformed variables
228 makes estimated effects of different glycans comparable, as these will have the same
229 standardized variance. False discovery rate (FDR) was controlled by the Benjamini-Hochberg

230 procedure at the specified level of 0.05. Data was analysed and visualized using R
231 programming language (version 3.5.2)(32).
232 *TwinsUK cohort*. Normalization of peak intensities to the total chromatogram area was
233 performed for each measured sample separately. Calculated proportions were then batch
234 corrected using ComBat method (R package *sva*)(31). After the batch correction the first 11
235 peaks, which predominantly originate from IgG (33), were used to calculate 6 derived glycan
236 traits – agalactosylation (G0), monogalactosylation (G1), digalactosylation (G2), bisecting
237 GlcNAc (B), core fucosylation (CF) and high mannose structures (HM). Mixed models were
238 fitted to estimate the effect of BMI change on IgG N-glycome (R package *lme4*)(34). Directly
239 measured or derived glycan trait was used as a dependent variable in the mixed model. To
240 differentiate between BMI change and the absolute BMI value, the variable was separated to
241 $BMI_{baseline}$ and $BMI_{difference}$ (calculated according to the following equation: $BMI_{difference} =$
242 $BMI_{follow\ up\ age} - BMI_{baseline\ age}$), and both were used in the model as a fixed effect. Since
243 IgG N-glycome is affected by aging, age was included both as a fixed effect and a random
244 slope. Finally, to meet the independency criteria, family ID and individual ID (nested within
245 family) were included in the model as a random intercept. Due to multiple model fitting (for
246 11 directly measured and 6 derived glycan traits) false discovery rate was controlled using
247 Benjamini-Hochberg method. All statistical analyses were performed using R programming
248 language (version 3.6.3)(32).
249
250 **RESULTS**
251 ***<u>Pre-surgical low-calorie diet extensively changes plasma N-glycome</u>***
252 We profiled both plasma and IgG N-glycome in a cohort of bariatric surgery-candidate patients
253 at the beginning and at the end of their pre-operative diet. We calculated corresponding
254 derived glycan traits, which average particular glycosylation features. By employing a linear
255 mixed model, we observed ample changes in plasma N-glycome, as 10 out of 16 calculated
256 derived traits displayed significant alterations after the low-calorie diet. Namely, low
257 branched (LB), agalactosylated (G0), monogalactosylated (G1), asialylated (S0),
258 monosialylated (S1), core fucosylated (CF) and glycans bearing a bisecting GlcNAc (B) showed
259 a substantial increase in their abundances (Table 3). Conversely, high branched (HB),
260 trisialylated (S3) and trigalactosylated (G3) glycan abundances decreased (Table 3).
261 Interestingly, IgG glycome was not affected by the low-calorie diet, as its derived traits did not

262 display any significant changes after the dieting period. Graphical representation of the
263 longitudinal alterations in plasma N-glycome after low calorie diet are depicted in Figure 1.

264 **Table 3 Low-calorie diet induces significant changes in plasma N-glycome**. Longitudinal
265 analysis was performed by implementing a linear mixed effects model, with time as a fixed
266 effect and the individual sample measurement as a random effect. False discovery rate was
267 controlled using Benjamini-Hochberg method at the specified level of 0.05.

Derived glycan trait	***Time_effect***	***Time_SE***	***Time_p-value***	***Adjusted p-value***
monogalactosylation (G1)	0.6020	0.0796	4.18×10^{-05}	6.69×10^{-04}
trisialylation (S3)	-1.1512	0.2008	3.04×10^{-04}	2.43×10^{-03}
agalactosylation (G0)	0.4903	0.0948	6.09×10^{-04}	2.44×10^{-03}
core fucosylation (CF)	0.5431	0.1011	4.73×10^{-04}	2.44×10^{-03}
high branching (HB)	-1.1925	0.2468	9.43×10^{-04}	2.52×10^{-03}
asialylation (S0)	0.6336	0.1310	9.40×10^{-04}	2.52×10^{-03}
trigalactosylation (G3)	-1.1925	0.2581	1.24×10^{-03}	2.84×10^{-03}
bisecting GlcNAc (B)	0.5457	0.1350	2.84×10^{-03}	5.69×10^{-03}
low branching (LB)	0.9839	0.3060	9.99×10^{-03}	1.78×10^{-02}
monosialylation (S1)	0.5024	0.1981	2.98×10^{-02}	4.77×10^{-02}
disialylation (S2)	-0.4314	0.1941	4.99×10^{-02}	7.25×10^{-02}
high mannose (HM)	0.7545	0.3619	6.24×10^{-02}	8.33×10^{-02}
antennary fucosylation (AF)	-0.1804	0.1102	1.28×10^{-01}	1.58×10^{-01}
digalactosylation (G2)	0.3107	0.2309	2.01×10^{-01}	2.30×10^{-01}
tetragalactosylation (G4)	-0.3446	0.3477	3.36×10^{-01}	3.58×10^{-01}
tetrasialylation (S4)	-0.3049	0.3547	4.00×10^{-01}	4.00×10^{-01}

268 Red – significant decrease; green – significant increase; blue – non-significant change.
269 GlcNAc – *N*-acetylglucosamine; SE – standard error

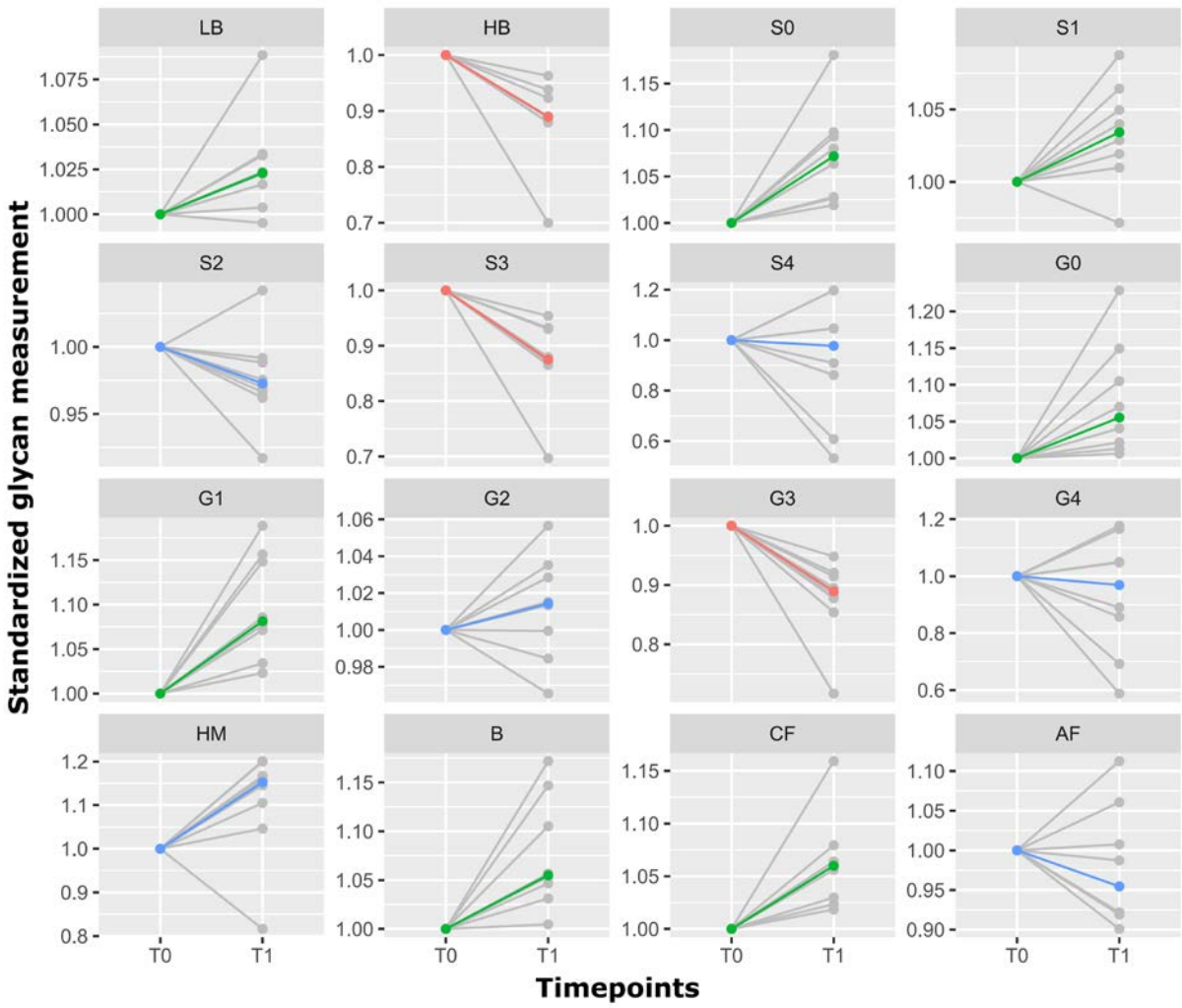

Figure 1 Low calorie diet-related alterations in plasma N-glycome after a 3-week follow-up. Red line – significant decrease; green line – significant increase; blue line – non-significant change.

<u>Bariatric surgery markedly alters IgG N-glycosylation</u>

Using the same chromatographic approach, we analysed samples from patients who underwent bariatric surgery. The plasma samples were collected on the day of surgery (month 0), approximately 6 months post-surgery and 12 months post-surgery. Both plasma and IgG N-glycans were profiled in each of these timepoints, and the obtained values were used for derived glycan traits calculations. Of the examined plasma glycosylation features, only agalactosylation (G0) displayed significant decrease after bariatric surgery (Table 4). On the other hand, IgG N-glycome showed more extensive changes, following the bariatric procedure. Namely, four out of eight tested derived traits showed marked changes: core fucosylated (CF) and agalactosylated (G0) glycans decreased, while digalactosylated (G2) and monosialylated (S1) glycans increased after the surgery (Table 4). The IgG glycans whose

285 abundances were increased after bariatric surgery are major components of a "young" IgG
286 glycome, as they are typically associated with a younger age. The opposite applies to
287 agalactosylated structures , which are usual denominators of an "old" IgG glycome profile. We
288 also examined the correlation of patients' clinical data with plasma and IgG glycome features
289 using multivariate analysis, but found no statistically significant associations (data not shown).
290 Finally, the type of bariatric surgery (either sleeve gastrectomy or Roux-en-Y gastric bypass)
291 did not affect plasma nor IgG glycome composition. Graphical representations of the
292 longitudinal alterations in IgG and plasma glycosylation features are depicted in Figure 2 and
293 Supplementary Figure 3, respectively.

294 **Table 4 Bariatric surgery induces significant changes in plasma and IgG N-glycomes.**
295 Longitudinal analysis was performed by implementing a linear mixed effects model, with
296 time as a fixed effect and the individual sample measurement as a random effect. False
297 discovery rate was controlled using Benjamini-Hochberg method at the specified level of
298 0.05.

N-glycome	***Derived glycan trait***	***Time_effect***	***Time_SE***	***Time_p-value***	***Adjusted p-value***
plasma	agalactosylation (G0)	-0.0273	0.0071	5.26×10^{-04}	8.42×10^{-03}
IgG	agalactosylation (G0)	-0.0339	0.0078	9.23×10^{-05}	7.38×10^{-04}
IgG	digalactosylation (G2)	0.0275	0.0072	3.75×10^{-04}	1.50×10^{-03}
IgG	monosialylation (S1)	0.0193	0.0080	1.97×10^{-02}	3.94×10^{-02}
IgG	core fucosylation (CF)	-0.0155	0.0064	1.74×10^{-02}	3.94×10^{-02}

299 Red – significant decrease; green – significant increase. SE – standard error.

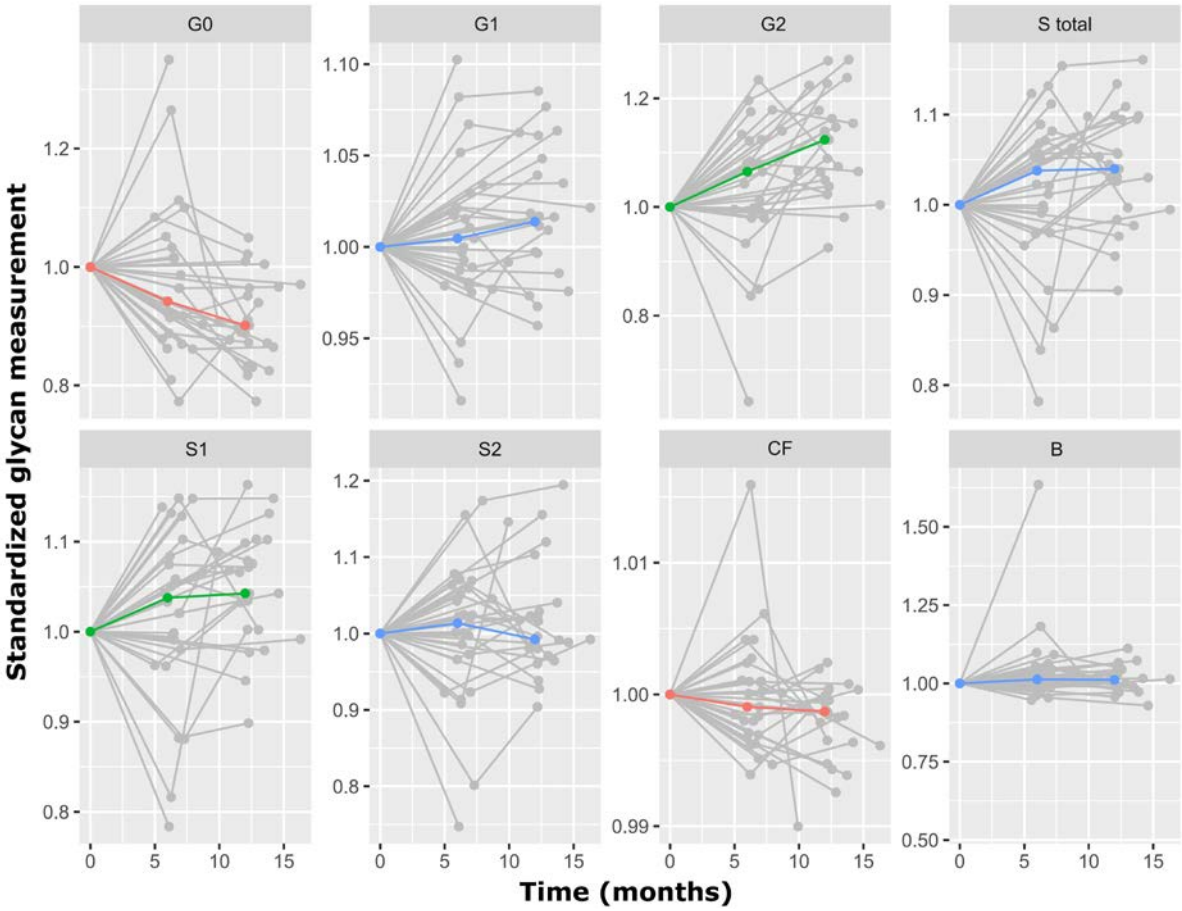

Figure 2 Bariatric surgery-related alterations in IgG N-glycome over time (months). Red line – significant decrease; green line – significant increase; blue line – non-significant change.

<u>Weight loss induces shift towards ''young'' IgG N-glycome</u>

Using the same chromatographic approach, we profiled plasma protein N-glycome from 1,680 TwinsUK study participants sampled at several timepoints over a 20-year-period. This served as a replication of the findings from the bariatric cohort, whose participants exhibited the reversal from ''old'' to ''young'' IgG N-glycome due to weight loss. As these results showed prominent changes in IgG composite glycan traits only, herein we focused on IgG glycosylation changes. Due to the fact that for TwinsUK cohort plasma glycome was profiled, we calculated derived traits and performed statistical analysis only on the first 11 glycan peaks, corresponding to the glycans predominantly originating from IgG (33). Six derived traits were calculated – agalactosylation (G0), monogalactosylation (G1), digalactosylation (G2), incidence of bisecting GlcNAc (B), core fucosylation (CF) and incidence of high mannose structures (HM). We examined IgG glycome alterations associated with changes in BMI using a mixed model on a subset of 3,742 samples. Out of six examined IgG glycosylation features (derived traits), three displayed significant BMI-related changes – agalactosylation (G0),

317 digalactosylation (G2) and incidence of high mannose structures (HM) (Table 5). Namely, the
318 abundance of digalactosylated (G2) glycans increased with the BMI decrease, while the
319 abundance of agalactosylated (G0) and high mannose glycans (HM) decreased with the weight
320 loss, estimated by the BMI drop. These findings are in line with the results observed in the
321 bariatric surgery cohort. Graphical representation of the longitudinal BMI-dependent
322 alterations of IgG glycosylation are depicted at Figure 3.

323 **Table 5 Longitudinally monitored weight loss results with significant changes of IgG N-**
324 **glycosylation.** Longitudinal analysis was performed by implementing a mixed model, fitted
325 to estimate the effect of BMI change on IgG N-glycome. False discovery rate was controlled
326 using Benjamini-Hochberg method at the specified level of 0.05.

Derived glycan trait	***BMI difference effect (glycan abundance (%) change per 1 kgm^{-2} decrease in BMI)***	***BMI difference SE (glycan abundance (%) change per 1 kgm^{-2} decrease in BMI)***	***p-value***	***Adjusted p-value***
digalactosylation (G2)	0.2004	0.0403	6.88×10^{-07}	5.85×10^{-06}
high mannose (HM)	-0.0519	0.0119	1.33×10^{-05}	5.66×10^{-05}
agalactosylation (G0)	-0.1048	0.0397	8.43×10^{-03}	1.79×10^{-02}
bisecting GlcNAc (B)	0.0526	0.0262	4.49×10^{-02}	6.94×10^{-02}
monogalactosylation (G1)	-0.0573	0.0343	9.53×10^{-02}	1.25×10^{-01}
core fucosylation (CF)	-0.0059	0.0285	8.36×10^{-01}	8.89×10^{-01}

327 Red – significant decrease; green – significant increase; blue – non-significant change.
328 GlcNAc – *N*-acetylglucosamine; SE – standard error

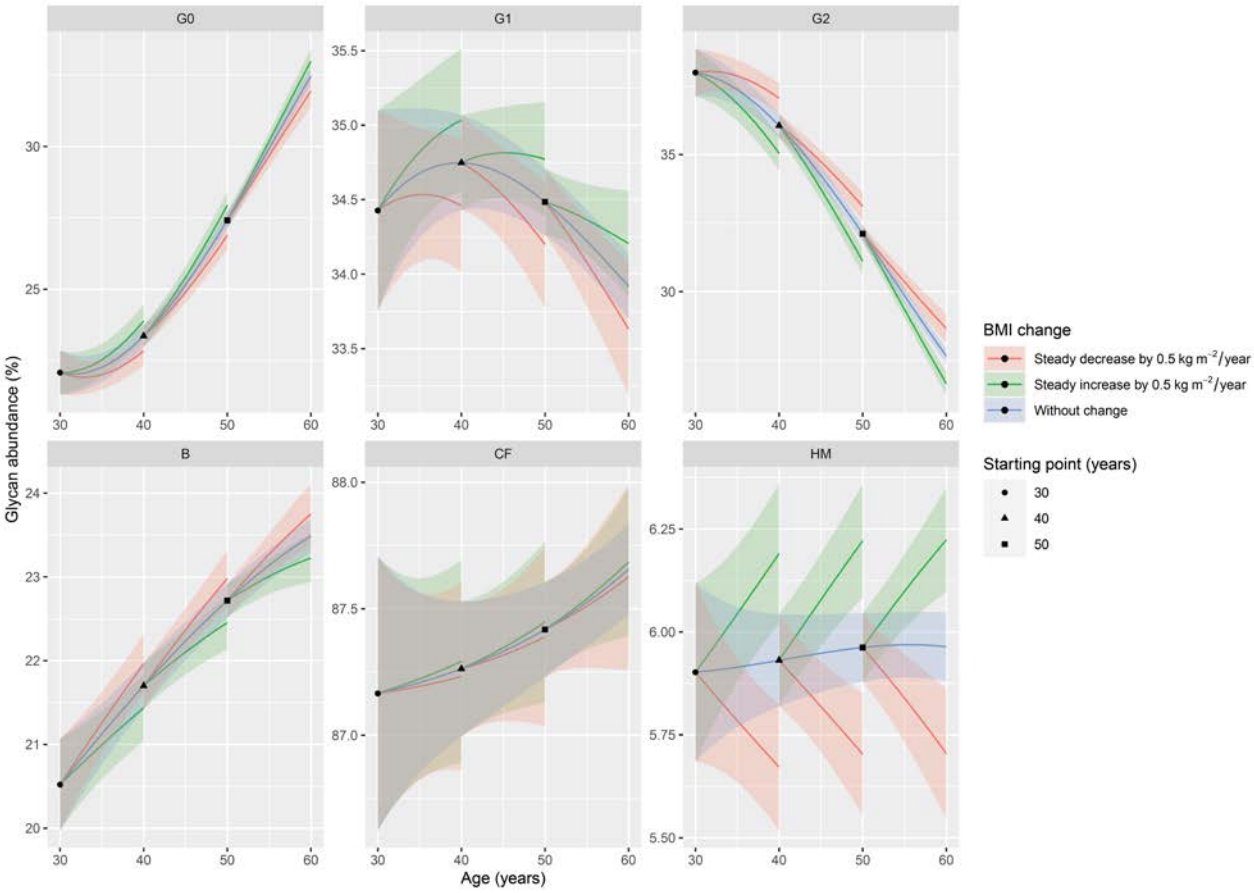

Figure 3 BMI-associated alterations in IgG N-glycosylation across multiple timepoints. Changes in IgG derived traits are presented with lineplots of hypothetical ageing of TwinsUK participants (all women). Black dot represents a starting point of a 30-year-old woman, black triangle of a 40-year-old woman and black square of a 50-year-old woman. All of these women have a baseline BMI of 25 kg m^{-2}. Blue lines represent age-related IgG glycosylation changes attributed to stabile BMI. Green lines represent age-related IgG glycosylation changes attributed to increasing BMI (0.5 kg m^{-2} per year, through a period of 10 years). Red lines represent age-related IgG glycosylation changes attributed to decreasing BMI (0.5 kg m^{-2} per year, through a period of 10 years). Highlighted areas represent 95% confidence intervals. The effect of age on IgG glycosylation is represented with the curve slope, while the effect of BMI change is represented with the distance of green/red line from the blue line.

DISCUSSION

In this study, we have observed extensive changes in both plasma and IgG N-glycome associated with weight loss following low-calorie diet and bariatric surgery, or expressed through BMI decrease. To the best of our knowledge, this is the first study to investigate

346 plasma and IgG N-glycome alterations in patients who underwent a low-calorie diet followed
347 by bariatric surgery.
348 Prior to bariatric surgery, patients were subjected to a low-calorie diet which caused
349 significant and extensive changes to the plasma protein N-glycome. The observed changes can
350 be summarized as significant increase in low-branched, biantennary structures (S0, S1, G0,
351 G1…) and, conversely, substantial decrease in high-branched, triantennary, more complex
352 structures (S3, G3). The glycosylation alterations induced by a low-calorie diet are showing
353 exactly the opposite direction of change than those seen in various inflammatory conditions,
354 such as type 2 diabetes, chronic obstructive pulmonary disease and inflammatory bowel
355 disease (17,30,35,36), suggesting a gradual attenuation of inflammation. Interestingly, no
356 significant changes were found for the IgG N-glycome alone after the diet, probably due to
357 the relatively short follow-up period (3 weeks), which matches IgG serum half-life. Altogether,
358 our glycomic data suggest that the overall inflammatory body status improves after a short
359 time of low-calorie diet, reflecting a quickly noticeable and beneficial metabolic effect.
360
361 We have analysed both plasma and IgG N-glycome from individuals who underwent bariatric
362 surgery, in a longitudinal manner. We observed significant changes in both plasma and IgG N-
363 glycome. In particular, plasma N-glycome showed significant alterations only in
364 agalactosylated (G0) glycans, whose abundance decreased during the follow-up period. Since
365 the majority of agalactosylated species in plasma originates from IgG (33), it is no surprise that
366 this glycosylation feature was also found to be significantly decreased in IgG glycome analysis.
367 Elevated levels of G0 IgG glycoforms are typically associated with aging, pro-inflammatory IgG
368 glycan profile and various inflammatory diseases (12). On the other hand, the levels of
369 digalactosylated (G2) glycans increased after bariatric surgery and at sequential timepoints, in
370 accordance with a reduced inflammatory potential of the circulating IgG. Interestingly, the
371 increased levels of IgG galactosylation are associated with a younger biological age and are
372 considered, in a way, as a measure of an individual's well-being (15). Converesely, IgG
373 galactosylation levels substantially decrease with ageing and during inflammation (12,14). Our
374 results demonstrate that weight loss, resulting from bariatric surgery, can initiate the reversal
375 from an ''old'' to a ''young'' IgG N-glycome, potentially reversing the clock for the
376 immune/biological age. Furthermore, bariatric surgery also resulted in significant IgG glycome
377 alteration inducing a decrease in core fucosylation. The vast majority of circulating IgG

378 molecules bears core fucose (approximately 95%), which profoundly decreases IgG binding
379 affinity to FcγRIIIA receptor and sequential antibody-dependent cellular cytotoxicity (ADCC)
380 (37). ADCC is largely mediated by natural killer cells that can lyse target cells and fight viral
381 infections. This would suggest that an extensive weight loss ameliorates immune responses
382 dedicated to combat viral infections, by altering IgG glycosylation and modulating its effector
383 functions. Lastly, bariatric surgery-related weight loss led to an increase in IgG sialylation,
384 which is the main modulator of the IgG anti-inflammatory actions (38). In addition to its anti-
385 inflammatory actions, the level of IgG sialylation has been implicated in the pathogenesis of
386 obesity-induced insulin resistance and hypertension, as already mentioned (23,24). Namely,
387 inhibitory IgG receptor FcγRIIB was found to be expressed in the microvascular endothelium.
388 Sequentially, it was shown that hyposialylated IgG acts as its operating ligand, leading to the
389 induction of obesity-related insulin resistance and hypertension. On the other hand, the
390 sialylated glycoform is not activating the signalling pathways responsible for the insulin
391 resistance and hypertension development, but is rather preserving insulin sensitivity and
392 normal vasomotor tone, even in obese mice. Interestingly, the same group made another
393 significant discovery – promotion of IgG sialylation breaks the link between obesity and
394 hypertension/insulin resistance (24,25). Namely, supplementation with the sialic acid
395 precursor restored IgG sialylation, highlighting a potential approach to improve both
396 metabolic and cardiovascular health in humans, with a single intervention. Our data suggest
397 that a similar effect might be achieved by weight loss interventions, through restoring of IgG
398 sialylation levels. Altogether, it is remarkable that such profound effects were observed on a
399 rather small number of participants, which further highlights their significance in a given
400 biological setting.
401
402 Lastly, in order to confirm the effects of weight loss on the biological/immune age, we
403 investigated how BMI decrease affects IgG N-glycome during a 20-year-period. We observed
404 the prominent inverse changes of agalactosylated (G0) and digalactosylated (G2) IgG glycans.
405 Namely, agalactosylated IgG glycans significantly decreased, while digalactosylated ones
406 substantially increased as the BMI decreased. These observations corroborated our earlier
407 findings, confirming that the body weight reduction reverses IgG glycome from “old” to
408 “young”, implying at the same time a likely reduction in the biological/ immune age.
409 Nonetheless, we have to acknowledge the following limitations of TwinsUK as a replication

410 cohort: first – TwinsUK participants have not experienced such an extensive weight loss, which
411 potentially influenced the replication of other significant glycan changes from the bariatric
412 cohort; second – herein, the weight loss was approximated by BMI decrease, which is usually
413 a legitimate assumption, however, it does not have to apply to all cases; and third – herein we
414 profiled plasma glycome, while the IgG glycan traits were only approximated and the
415 information on IgG sialylation was confounded by other plasma glycoproteins. Ideally, these
416 issues could be circumvented in the future studies whose experimental design would allow
417 the simultaneous, multi-centre follow-up of larger groups of patients.
418 Intense physical exercise can also shift IgG N-glycome towards a ”younger” profile by
419 increasing IgG galactosylation (26). Although another study reported that prolonged intensive
420 exercise can have the opposite effect and promote pro-inflammatory changes of IgG N-
421 glycome (39), its findings are not surprising since it recruited healthy, normal-weight female
422 participants, subjected to the intense energy deprivation and exercise levels, to induce
423 substantial fat loss in a rather short time period. The authors also highlighted that starting
424 weight and the way in which weight loss is achieved could be crucial for the final effect on the
425 immune system. Therefore, it seems that exercise overall has a positive impact on the immune
426 system and biological clock, but its intensity and duration should be personalized in order to
427 provide the optimal results.
428 To summarize, our results indicate that weight loss has impact on inflammation and biological
429 aging by altering plasma and IgG N-glycosylation patterns. Glycosylation changes can be
430 reliably quantified and used to estimate the “age” of the immune system. This could represent
431 a valuable tool in the context of COVID-19 patient stratification. Since inter-individual
432 variation in protein glycosylation is extensive, its functional implications on membrane
433 expression of various proteins (including ACE2), functional properties of newly synthesized
434 SARS-CoV-2 virus particles and regulation of the immune responses may also explain severe
435 cases of COVID-19 in apparently healthy individuals. A previous research showed that
436 impairment of ACE2 N-glycosylation affects its ability to allow the transduction of SARS Human
437 coronavirus NL63 (HCoV-NL63) particles, by disrupting the viral endocytosis (40).
438 Future glycomic studies of patients infected with SARS-CoV-2 would help to elucidate whether
439 ACE2 N-glycosylation differs in patients with severe COVID-19, compared to asymptomatic
440 patients or healthy individuals. For the time being, it appears that severity of COVID-19
441 associates with the majority of obesity-related comorbidity risk factors (41). Therefore, by

442 improving metabolic and endocrine health through weight loss, which consequently
443 contributes to the preservation of a healthy immune system, one has a best chance to fight
444 infections.
445
446 **ACKNOWLEDGMENTS**
447 This research was funded by the National Institute for Health Research (NIHR) Oxford
448 Biomedical Research Centre (BRC). The views expressed are those of the author(s) and not
449 necessarily those of the NHS, the NIHR or the Department of Health. The authors thank Rachel
450 Franklin, Michelle Haylock, James Chivenga, Roxanne Williams and the BRC Oxford GI Biobank
451 for sample collection. The authors thank all the patients who took part in this study.
452
453 **FUNDING**
454 Glycosylation analysis was performed in Genos Glycoscience Research Laboratory and partly
455 supported by the European Union's Horizon 2020 grants Backup (grant# 777090), European
456 Structural and Investment Funds IRI grant (#KK.01.2.1.01.0003), Centre of Competence in
457 Molecular Diagnostics (#KK.01.2.2.03.0006) and Croatian National Centre of Research
458 Excellence in Personalized Healthcare grant (#KK.01.1.1.01.0010). Bariatric research was
459 supported by the National Institute for Health Research (NIHR) Oxford Biomedical Research
460 Centre Gastroenterology and Mucosal Immunity Theme to CVA-C and VLG, Oxford Biomedical
461 Research Centre Diabetes and Metabolism theme for JWT, MRC programme grant to JWT (ref.
462 MR/P011462/1), the NIHR Research Capability Funding to VLG and AG, the Wellcome Trust
463 (101734/Z/13/Z) to AG. NJD is supported by a University of Oxford Novo Nordisk Clinical
464 Research Fellowship. TwinsUK received funding from the Wellcome Trust European
465 Community's Seventh Framework Programme (FP7/2007-2013 to TwinsUK); the National
466 Institute for Health Research (NIHR) Clinical Research Facility at Guy's & St Thomas' NHS
467 Foundation Trust and the Nottingham NIHR Biomedical Research Centre based at Guy's and
468 St Thomas' NHS Foundation Trust and King's College London. CM is funded by the MRC AimHy
469 (MR/M016560/1) project grant and by the Chronic Disease Research Foundation.
470
471 **AUTHOR`S CONTRIBUTION**
472 Study design: CM, AG, CVA-C, GL. Data collection: VLG, ACv, TŠ, NJD, ACi, HD, MF, CM. Data
473 analysis: DK, FV. Data interpretation: VLG, ACv, TŠ, NJD, DK, FV, MF, JWT, OG, TS, CM, AG,

CVA-C, GL. Drafting manuscript: VLG, ACv, TŠ, NJD, DK, FV, GL. Revising and approving final version of manuscript: ALL. CM, AG, CVA-C and GL take responsibility for the integrity of the data analysis

REFERENCES

1. Obesity and overweight [Internet]. [cited 2020 Apr 16]. Available from: https://www.who.int/news-room/fact-sheets/detail/obesity-and-overweight

2. Petrilli CM, Jones SA, Yang J, Rajagopalan H, O'Donnell LF, Chernyak Y, et al. Factors associated with hospitalization and critical illness among 4,103 patients with COVID-19 disease in New York City. medRxiv. 2020 Apr 11;2020.04.08.20057794.

3. Garg S. Hospitalization Rates and Characteristics of Patients Hospitalized with Laboratory-Confirmed Coronavirus Disease 2019 — COVID-NET, 14 States, March 1–30, 2020. MMWR Morb Mortal Wkly Rep [Internet]. 2020 [cited 2020 Apr 26];69. Available from: https://www.cdc.gov/mmwr/volumes/69/wr/mm6915e3.htm

4. Han TS, Lean ME. A clinical perspective of obesity, metabolic syndrome and cardiovascular disease. JRSM Cardiovasc Dis. 2016 Dec;5:2048004016633371.

5. Alpert A, Pickman Y, Leipold M, Rosenberg-Hasson Y, Ji X, Gaujoux R, et al. A clinically meaningful metric of immune age derived from high-dimensional longitudinal monitoring. Nat Med. 2019 Mar;25(3):487–95.

6. Franceschi C, Garagnani P, Parini P, Giuliani C, Santoro A. Inflammaging: a new immune–metabolic viewpoint for age-related diseases. Nature Reviews Endocrinology. 2018 Oct;14(10):576–90.

7. Touch S, Clément K, André S. T Cell Populations and Functions Are Altered in Human Obesity and Type 2 Diabetes. Curr Diab Rep. 2017 Sep;17(9):81.

8. Dhurandhar NV, Bailey D, Thomas D. Interaction of obesity and infections. Obes Rev. 2015 Dec;16(12):1017–29.

9. Lauc G, Sinclair D. Biomarkers of biological age as predictors of COVID-19 disease severity. Aging [Internet]. 2020 Apr 8 [cited 2020 Apr 14]; Available from: http://www.aging-us.com/article/103052/text

10. Lauc G, Pezer M, Rudan I, Campbell H. Mechanisms of disease: The human N-glycome. Biochimica et Biophysica Acta - General Subjects. 2016;1860(8):1574–82.

11. Gornik O, Pavić T, Lauc G. Alternative glycosylation modulates function of IgG and other proteins - implications on evolution and disease. Biochim Biophys Acta. 2012 Sep;1820(9):1318–26.

12. Gudelj I, Lauc G, Pezer M. Immunoglobulin G glycosylation in aging and diseases. Cellular Immunology. 2018;

13. Dall'Olio F. Glycobiology of aging. In: Subcellular Biochemistry. 2018.

14. Krištić J, Vučković F, Menni C, Klarić L, Keser T, Beceheli I, et al. Glycans Are a Novel Biomarker of Chronological and Biological Ages. The Journals of Gerontology: Series A. 2014 Jul;69(7):779–89.

515 15. Štambuk J, Nakić N, Vučković F, Pučić-Baković M, Razdorov G, Trbojević-Akmačić I, et al.
516 Global variability of the human IgG glycome [Internet]. Biochemistry; 2019 Feb [cited
517 2020 Jan 31]. Available from: http://biorxiv.org/lookup/doi/10.1101/535237

518 16. Menni C, Gudelj I, MacDonald-Dunlop E, Mangino M, Zierer J, Bešić E, et al.
519 Glycosylation Profile of Immunoglobulin G Is Cross-Sectionally Associated with
520 Cardiovascular Disease Risk Score and Subclinical Atherosclerosis in Two Independent
521 Cohorts. Circulation Research. 2018;122(11):1555–64.

522 17. Wittenbecher C, Štambuk T, Kuxhaus O, Rudman N, Vučković F, Štambuk J, et al. Plasma
523 N-Glycans as Emerging Biomarkers of Cardiometabolic Risk: A Prospective Investigation
524 in the EPIC-Potsdam Cohort Study. Diabetes Care. 2020 Jan 7;43(3):661–8.

525 18. Gao Q, Dolikun M, Stambuk J, Wang H, Zhao F, Yiliham N, et al. Immunoglobulin G N-
526 Glycans as Potential Postgenomic Biomarkers for Hypertension in the Kazakh
527 Population. Omics. 2017;21(7):380–9.

528 19. Liu J, Dolikun M, Štambuk J, Trbojević-Akmačić I, Zhang J, Wang H, et al. The association
529 between subclass-specific IgG Fc N-glycosylation profiles and hypertension in the
530 Uygur, Kazak, Kirgiz, and Tajik populations. J Hum Hypertens. 2018 Sep;32(8–9):555–63.

531 20. Wang Y, Klarić L, Yu X, Thaqi K, Dong J, Novokmet M, et al. The Association Between
532 Glycosylation of Immunoglobulin G and Hypertension: A Multiple Ethnic Cross-Sectional
533 Study. Medicine. 2016 Apr;95(17):e3379.

534 21. Nikolac Perkovic M, Pucic Bakovic M, Kristic J, Novokmet M, Huffman JE, Vitart V, et al.
535 The association between galactosylation of immunoglobulin G and body mass index.
536 Progress in Neuro-Psychopharmacology and Biological Psychiatry. 2014 Jan;48:20–5.

537 22. Russell AC, Kepka A, Trbojević-Akmačić I, Ugrina I, Song M, Hui J, et al. Increased central
538 adiposity is associated with pro-inflammatory immunoglobulin G N-glycans.
539 Immunobiology. 2019;224(1):110–5.

540 23. Sundgren NC, Vongpatanasin W, Boggan BMD, Tanigaki K, Yuhanna IS, Chambliss KL, et
541 al. IgG receptor FcγRIIB plays a key role in obesity-induced hypertension. Hypertension.
542 2015 Feb 21;65(2):456–62.

543 24. Tanigaki K, Sacharidou A, Peng J, Chambliss KL, Yuhanna IS, Ghosh D, et al.
544 Hyposialylated IgG activates endothelial IgG receptor Fc**γ**RIIB to promote obesity-
545 induced insulin resistance. J Clin Invest. 2018 Jan 2;128(1):309–22.

546 25. Peng J, Vongpatanasin W, Sacharidou A, Kifer D, Yuhanna IS, Banerjee S, et al.
547 Supplementation with the Sialic Acid Precursor N-acetyl-D-Mannosamine Breaks the
548 Link Between Obesity and Hypertension. 2019.

549 26. Tijardović M, Marijančević D, Bok D, Kifer D, Lauc G, Gornik O, et al. Intense Physical
550 Exercise Induces an Anti-inflammatory Change in IgG N-Glycosylation Profile. Frontiers
551 in Physiology. 2019;10(December):1–10.

552 27. Nguyen NT, Kim E, Vu S, Phelan M. Ten-year Outcomes of a Prospective Randomized
553 Trial of Laparoscopic Gastric Bypass Versus Laparoscopic Gastric Banding. Ann Surg.
554 2018;268(1):106–13.

555 28. O'Brien P. Bariatric surgery and type 2 diabetes: a step closer to defining an optimal
556 approach. The Lancet Diabetes & Endocrinology. 2019 Dec 1;7(12):889–91.

557 29. Verdi S, Abbasian G, Bowyer RCE, Lachance G, Yarand D, Christofidou P, et al. TwinsUK:
558 The UK Adult Twin Registry Update. Twin Res Hum Genet. 2019 Dec;22(6):523–9.

559 30. Pavić T, Dilber D, Kifer D, Selak N, Keser T, Ljubičić Đ, et al. N-glycosylation patterns of
560 plasma proteins and immunoglobulin G in chronic obstructive pulmonary disease. J
561 Transl Med. 2018 Nov 21;16.

562 31. Leek JT, Johnson WE, Parker HS, Jaffe AE, Storey JD. The sva package for removing
563 batch effects and other unwanted variation in high-throughput experiments.
564 Bioinformatics. 2012 Mar 15;28(6):882–3.

565 32. R Core Team (2020). R: A language and environment for statistical computing. R
566 Foundation for Statistical Computing, Vienna, Austria. URL https://www.R-
567 project.org/.

568 33. Clerc F, Reiding KR, Jansen BC, Kammeijer GSM, Bondt A, Wuhrer M. Human plasma
569 protein N-glycosylation. Glycoconj J. 2016 Jun 1;33(3):309–43.

570 34. Bates D, Mächler M, Bolker B, Walker S. Fitting Linear Mixed-Effects Models Using
571 lme4. Journal of Statistical Software. 2015 Oct 7;67(1):1–48.

572 35. Clerc F, Novokmet M, Dotz V, Reiding KR, de Haan N, Kammeijer GSM, et al. Plasma N-
573 Glycan Signatures Are Associated With Features of Inflammatory Bowel Diseases.
574 Gastroenterology. 2018;155(3):829–43.

575 36. Novokmet M, Lukić E, Vučković F, –Durić Ž, Keser T, Rajšl K, et al. Changes in IgG and
576 total plasma protein glycomes in acute systemic inflammation. Scientific Reports. 2014
577 Mar 11;4(1):1–10.

578 37. Iida S, Kuni-Kamochi R, Mori K, Misaka H, Inoue M, Okazaki A, et al. Two mechanisms of
579 the enhanced antibody-dependent cellular cytotoxicity (ADCC) efficacy of non-
580 fucosylated therapeutic antibodies in human blood. BMC Cancer. 2009 Feb 18;9:58.

581 38. Kaneko Y, Nimmerjahn F, Ravetch JV. Anti-Inflammatory Activity of Immunoglobulin G
582 Resulting from Fc Sialylation. Science. 2006 Aug 4;313(5787):670–3.

583 39. Sarin HV, Gudelj I, Honkanen J, Ihalainen JK, Vuorela A, Lee JH, et al. Molecular
584 Pathways Mediating Immunosuppression in Response to Prolonged Intensive Physical
585 Training, Low-Energy Availability, and Intensive Weight Loss. Front Immunol.
586 2019;10:907.

587 40. Zhao X, Guo F, Comunale MA, Mehta A, Sehgal M, Jain P, et al. Inhibition of
588 endoplasmic reticulum-resident glucosidases impairs severe acute respiratory

589 syndrome coronavirus and human coronavirus NL63 spike protein-mediated entry by
590 altering the glycan processing of angiotensin I-converting enzyme 2. Antimicrob Agents
591 Chemother. 2015 Jan;59(1):206–16.

592 41. Maffetone PB, Laursen PB. The Perfect Storm: Coronavirus (Covid-19) Pandemic Meets
593 Overfat Pandemic. Front Public Health [Internet]. 2020 [cited 2020 Apr 24];8. Available
594 from:
595 https://www.frontiersin.org/articles/10.3389/fpubh.2020.00135/full?utm_source=F-
596 NTF&utm_medium=EMLX&utm_campaign=PRD_FEOPS_20170000_ARTICLE

597